PCCP

PAPER

View Article Online
View Journal | View Issue

Cite this: *Phys. Chem. Chem. Phys.*, 2017, **19**, 4827

Kinetics, mechanisms and ionic liquids in the uptake of *n*-butylamine onto low molecular weight dicarboxylic acids

Michelle C. Fairhurst,[a] Michael J. Ezell,[a] Carla Kidd,[a] Pascale S. J. Lakey,[b] Manabu Shiraiwa[a] and Barbara J. Finlayson-Pitts*[a]

Received 19th December 2016,
Accepted 24th January 2017

DOI: 10.1039/c6cp08663b

rsc.li/pccp

Atmospheric particles adversely affect visibility, health, and climate, yet the kinetics and mechanisms of particle formation and growth are poorly understood. Multiphase reactions between amines and dicarboxylic acids (diacids) have been suggested to contribute. In this study, the reactions of *n*-butylamine (BA) with solid C3–C8 diacids were studied at 296 ± 1 K using a Knudsen cell interfaced to a quadrupole mass spectrometer. Uptake coefficients for amines on the diacids with known geometric surface areas were measured at initial amine concentrations from (3–50) × 10^{11} cm^{-3}. Uptake coefficients ranged from 0.7 ± 0.1 (2σ) for malonic acid (C3) to $<10^{-6}$ for suberic acid (C8), show an odd–even carbon number effect, and decrease with increasing chain length within each series. Butylaminium salts formed from evaporation of aqueous solutions of BA with C3, C5 and C7 diacids (as well as C8) were viscous liquids, suggesting that ionic liquids (ILs) form on the surface during the reactions of gas phase amine with the odd carbon diacids. Predictions from the kinetic multi-layer model of aerosol surface and bulk chemistry (KM-SUB) were quantitatively consistent with uptake occurring *via* dissolution of the underlying diacid into the IL layer and reaction with amine taken up from the gas phase. The butylaminium salts formed from the C4 and C6 diacids were solids, and their uptake coefficients were smaller. These experiments and kinetic modeling demonstrate the unexpected formation of ILs in a gas–solid reaction, and suggest that ILs should be considered under some circumstances in atmospheric processes.

Introduction

Secondary organic aerosol (SOA) particles are formed in the atmosphere from the oxidation of gas phase anthropogenic and biogenic compounds,[1–7] producing lower volatility compounds. These products can form new particles or can condense onto existing particles, causing them to grow.[8–10] At and above ~100 nm, particles scatter light efficiently, reducing visibility,[11,12] and they can also act as cloud condensation nuclei,[13–16] affecting climate and air quality.[17–21] Inhalation and deposition of particles into the human respiratory system[22–26] can cause deleterious health effects[17,25–34] including increased mortality.[28,35–37] Understanding the kinetics and mechanisms governing particle growth is thus very important.

Partitioning of gases into particles is dependent on physical properties of the particles, such as particle phase state.[38–40] If the particle is a low viscosity liquid, it will rapidly establish thermodynamic equilibrium with the gas phase.[4,38–47] However, recent studies have shown that under some conditions, SOA particles can exist in a more viscous or semi-solid phase.[48–60] In the extreme case of very high viscosity, this results in an essentially irreversible, diffusion limited, kinetic condensation mechanism for particle growth.[1,2,39]

Particles in the atmosphere can also grow *via* heterogeneous chemistry involving existing particles. For example, one reaction that can contribute to particle growth is that of acids with bases, either in the bulk and/or at the surface of particles. While the reactions of the inorganic acids H_2SO_4 and HNO_3 with ammonia and amines are well known,[8,61–75] amines are known to react with organic acids and diacids to form aminium salts,[76–78] and have been proposed to play a significant role in nanoparticle growth.[10,79] Amines are ubiquitous in the atmosphere, with their main sources stemming from agricultural and industrial processes, marine-life, and biomass burning.[80] Both carboxylic acids and dicarboxylic acids (diacids) are found in particles in many locations around the world.[81–88] Relevant to this, carboxylates and aminium ions have been shown to coexist in atmospheric particles.[89–91]

We report here the results of studies of the uptake of gaseous *n*-butylamine on a series of solid diacids (C3–C8; $HOOC(CH_2)_nCOOH$, where n = 1–6) in a Knudsen cell at 296 ± 1 K. In addition to

[a] *Department of Chemistry, University of California, Irvine, CA 92697, USA. E-mail: bjfinlay@uci.edu; Fax: +1 (949) 824-2420; Tel: +1 (949) 824-7670*
[b] *Max Planck Institute for Chemistry, Multiphase Chemistry Department, Hahn-Meitner-Weg 1, 55128 Mainz, Germany*

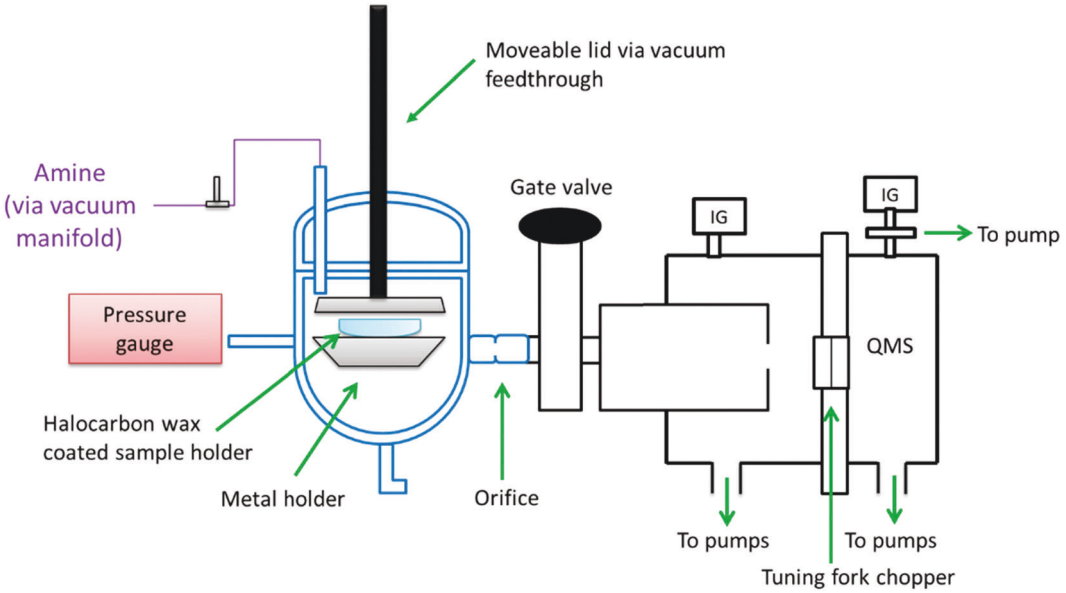

Fig. 1 Schematic of the Knudsen cell – quadrupole mass spectrometer (QMS). IG = ion gauge.

being found in the atmosphere, diacids are of great fundamental interest due to differences in properties that occur based on carbon chain length.[92–97] The behavior of the uptake coefficients with time and concentration, combined with additional probes of the nature of the salts formed from diacid–amine aqueous solutions, also provide insights into the mechanisms involved. These were tested using the kinetic multi-layer model of aerosol surface and bulk chemistry (KM-SUB),[98] which quantitatively reproduced the key experimental findings and confirmed the physical insights provided by the experimental data.

Experimental

Knudsen cell experiments

Experiments were carried out using a Knudsen cell interfaced to a quadrupole mass spectrometer (QMS, Extrel Core Mass Spectrometers) which has been described in detail previously.[99] The Knudsen cell was interfaced to the QMS using orifices with diameters of either 1.40 or 6.28 mm (Fig. 1), measured using dial calipers. Total pressure in the cell was measured using an APG100-XLC pressure gauge (Edwards) with an active gauge controller (Edwards) and was maintained at $\leq$0.3 mTorr to stay in the free molecular regime.[100–102] All experiments were performed at ambient temperature (296 $\pm$ 1 K). A modified Petri dish, coated with halocarbon wax (Halocarbon Products Corporation, Series 1500), was used to hold the diacid crystals. Malonic acid (C3), succinic acid (C4), glutaric acid (C5), adipic acid (C6), pimelic acid (C7), and suberic acid (C8) (Fig. 2), all with a stated purity of $\geq$99% (Sigma-Aldrich), were sieved using two mesh sizes (U.S. Standard) and the crystals which passed through the larger mesh, but not the smaller, were used. This gave average crystal sizes over a narrower size range than from unsieved samples (Table 1). Sieves used in

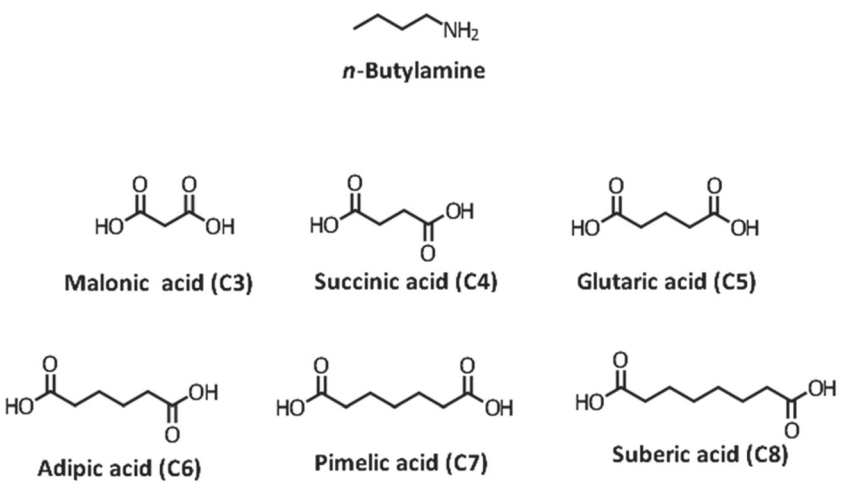

Fig. 2 Structures of *n*-butylamine (BA) and C3–C8 dicarboxylic acids (diacids) reactants.

Table 1 Sieve sizes and corresponding average lengths of each diacid crystal. Average lengths were derived from a sample size of 20 crystals

Diacid	Sieve sizes (μm)	Length ± 2σ (μm)
Malonic (C3)	425–500	519 ± 222
Succinic (C4)	425–500	443 ± 114
Glutaric (C5)	500–850	856 ± 338
Adipic (C6)	125–250	173 ± 82
Pimelic (C7)	500–850	742 ± 326
Suberic (C8)	125–250	132 ± 86

these experiments gave particles with average sizes in the range from 132 to 856 μm, depending on the diacid.

For all experiments, the solid diacid crystals formed less than a monolayer of crystals on the sample holder. The diacids were isolated from the rest of the cell by a moveable lid mounted on a vacuum feedthrough that could be raised to expose, or lowered to isolate, the diacid from the amine. Before the introduction of amine, each diacid sample was pumped on for 20 minutes to remove loosely bound water.

Introduction of the amine into the Knudsen cell was accomplished *via* a vacuum manifold. For experiments at (3–5) × 10^{12} cm^{-3} *n*-butylamine (BA), liquid BA (Sigma-Aldrich, 99%) was placed in a 50 mL bulb and underwent three freeze–pump–thaw cycles before filling the manifold and an attached 5 L evacuated bulb with gas phase BA. Experiments performed at concentrations of (3–5) × 10^{11} cm^{-3} BA involved diluting pure gas phase BA in helium (Praxair, 99.999%) in the 5 L bulb. The gas phase amine was introduced into the cell *via* a stainless steel needle valve and allowed to condition the cell and QMS until a steady signal was observed in the mass spectrum. The volume of the manifold and mixing bulb was sufficiently large that no drop in the monitored driving pressure was observed with the needle valve open during the course of these experiments.

The beam of amine molecules exiting the cell through the orifice was chopped with an 800 Hz tuning fork chopper (American Time Products, L40CB, model 5AR driver,) connected to a lock-in amplifier (Princeton-Applied Research, Model 5209). This allows for only those components that are chopped at 800 Hz to be measured by the lock-in amplifier, thus improving signal-to-noise. Operation of the mass spectrometer was controlled using Merlin Automation Data System software (Extrel, Version 3.0). The amine signal was monitored using the $H_2C{=}NH_2^+$ fragment ion at *m*/*z* 30.[103]

Uptake coefficients (γ) were calculated using eqn (1)[1,100] by monitoring the background corrected signal intensity of the amine when the moveable lid was closed (I_0) to cover the diacid sample and the signal intensity when the lid was opened (I_r) to expose the diacid to the amine:

$$\gamma = \left(\frac{I_0}{I_r} - 1\right)\left(\frac{A_{orifice}}{A_{surf}}\right) \quad (1)$$

$A_{orifice}$ and A_{surf} are the areas of the orifice and diacid surface area, respectively. Note that these are effective uptake coefficients that are calculated using assumed geometric crystal surface areas. As discussed below, the actual reactive surface areas may be different.

By measuring the average length of 20 sieved diacid crystals with dial calipers, and assuming a cubic structure with five sides that can react, the average exposed surface area of a single crystal was estimated. The total surface area was then calculated using the average exposed surface area for one crystal multiplied by the total number of crystals for each sample. For C3, C4, C5, and C7 diacids, the total number of crystals in an experiment was calculated from the measured total mass (Sartorius scale model 1702, ±0.0001 g) of diacid and the average mass per crystal. The mass per crystal was derived separately by counting the number of crystals used to obtain a measured mass of the order of 0.01 g. However, for adipic (C6) and suberic (C8) acids, the crystals were much smaller in size and photographs of the samples of mass ~0.01 g were used to physically count the number of crystals and thus obtain the average mass per crystal.

Sources of uncertainties in the calculated uptake coefficient arise in the variability of the signal intensities, the number of crystals, and the measured diameters of the orifices. However, the major source of uncertainty was the estimated total exposed surface area, which is dependent on the average measured size of sieved crystals and the assumption of a cubic crystal with five sides exposed for reaction. As shown in Table 1, the 2σ uncertainties in crystal size are as large as 65%. In addition, if crystals were assumed to be spherical instead of cubic, the surface area would be smaller by 60%, resulting in a corresponding increase in uptake coefficient. All sources of uncertainty were treated as independent and the cumulative uncertainty in the uptake coefficient was determined using propagation of errors.[104]

Butylaminium dicarboxylate salt formation; viscosity measurements

Evaporation of aqueous mixtures of amines with C2, C3, and C5 monocarboxylic acids have been previously shown to form ionic liquids.[77] In order to determine whether or not BA and dicarboxylic acids form ionic liquids, 2 : 1 and 1 : 1 molar ratios of aqueous BA : diacid mixtures were prepared in nanopure water (18 MΩ cm). Solutions were placed in a rotovap (Wheaton, SPIN-VAP) where solvent was evaporated off at 80–90 °C. The resulting extracts were stored under either nitrogen (Praxair, 99.999%) or ultra-zero air (Praxair). As described below, these procedures resulted in solid salts in some cases, and viscous liquids in others.

For mixtures resulting in liquids, viscosity was measured using the falling sphere viscometer technique. Briefly, the liquid is placed in a graduated cylinder and a 4.36 mm metal sphere of known density (7.96 × 10^3 kg m^{-3}) was allowed to fall through the liquid. The relationship between velocity of the falling sphere and viscosity of the liquid is given by eqn (2),[105]

$$\mu = \frac{2gr^2(\rho_s - \rho_f)}{9v} \quad (2)$$

where μ is the viscosity of the fluid (Pa s), g is the gravitational constant (9.8 m s^{-2}), r is the radius of the sphere (m), ρ_s and ρ_f are the densities of the sphere and fluid (kg m^{-3}), respectively, and v is the velocity of the sphere falling through the liquid (m s^{-1}). Videos of the sphere falling through the viscometer next to a ruler and stopwatch were recorded. Playback of the

Table 2 Parameters used in the KM-SUB model[98]

Parameter	Description	Value
$k_{1,b,GA}$	Bulk rate constant for reaction (R1) for glutaric acid (C5)	9×10^{-17} cm^3 s^{-1}
$k_{2,b,GA}$	Bulk rate constant for reaction (R2) for glutaric acid (C5)	$<5 \times 10^{-20}$ cm^3 s^{-1}
$k_{1,s,GA}$	Surface rate constant for reaction (R1) for glutaric acid (C5)	9×10^{-11} cm^2 s^{-1}
$k_{2,s,GA}$	Surface rate constant for reaction (R2) for glutaric acid (C5)	$<5 \times 10^{-20}$ cm^2 s^{-1}
$k_{1,b,AA}$	Bulk rate constant for reaction (R1) for adipic acid (C6)	2×10^{-22} cm^3 s^{-1}
$k_{1,s,AA}$	Surface rate constant for reaction (R1) for adipic acid (C6)	2×10^{-16} cm^2 s^{-1}
$\nu_{GA,AA}$	Viscosity of glutaric acid (C5) and adipic acid (C6)	1×10^9 Pa s
$\nu_{p1(GA)}$	Viscosity of Product 1 for the glutaric acid (C5) reaction system	1.3 Pa s
$\nu_{p2(GA)}$	Viscosity of Product 2 for the glutaric acid (C5) reaction system (see Table 4)	39 Pa s
$\nu_{p1(AA)}$	Viscosity of Product 1 for the adipic acid (C6) reaction system	1×10^9 Pa s
$\tau_{d,BA}$	Desorption lifetime	1×10^{-3} s
$\alpha_{s,BA}$	Surface accommodation coefficient of *n*-butylamine	0.3 (0.1 for Fig. 10a, see text)
H_{BA}	Henry's law constant of *n*-butylamine	1×10^{-5} mol cm^{-3} atm^{-1}

videos in slow-motion allowed for determination of the sphere's velocity by recording the distance travelled and the time. The density of the fluid was calculated separately from the measured mass of the liquid and the volume measured in a graduated cylinder.

Modeling studies

The gas phase concentration dependence of BA was investigated using the kinetic multi-layer model of aerosol surface and bulk chemistry (KM-SUB).[98] The model treats the following processes explicitly: adsorption and desorption of BA from the surface of the diacid, chemical reactions at the surface and in the bulk, and diffusion of reactants and products in the bulk. The model treats the condensed phase with a number of layers: a sorption layer, a quasi-static surface layer with a monolayer thickness, and 500 bulk layers which each had a 30 nm thickness. Sensitivity studies confirmed that the modeling results are practically the same if the number of bulk layers is above 100. Two reactions were included in the model as shown below:

$$\text{Diacid} + \text{BA} \xrightarrow{k_1} \text{Product 1} \quad \text{(R1)}$$

$$\text{Product 1} + \text{BA} \xrightarrow{k_2} \text{Product 2} \quad \text{(R2)}$$

For even carbon diacids it was assumed that Product 1 was solid and unreactive, while for the odd carbon diacids Product 1 is assumed to have lower viscosity and can further react with BA forming Product 2. The rate coefficients (k_1 and k_2) as well as the other kinetic parameters used in this study to model the experimental data are summarized in Table 2. These parameters include the surface accommodation coefficient, the desorption lifetime and the viscosity of the reactants and products. These parameters were varied systematically and iteratively to fit to the experimental data. Note that k_2 was constrained only with an upper limit, as viscosity measurements show that the viscosity of Product 2 (presumably the salt with stoichiometry of 2 : 1 amine to diacid) is higher than that of Product 1. This is consistent with the measurements described below of viscosities for salts formed with 2 : 1 and 1 : 1 amine : diacid ratios, where the viscosities for the 2 : 1 mixture were consistently larger than for the corresponding 1 : 1 salt (Table 4). Note however, that these are overall stoichiometries and the salt may consist of a mixture of the 1 : 1 salt, unreacted diacid, and possibly the 2 : 1 salt as well.

The viscosity in the bulk was calculated using an Arrhenius approach as shown below, using eqn (3),[106,107]

$$\text{Viscosity} = \exp(\textstyle\sum x_i \log(\nu_i)) \quad (3)$$

where x_i is the fraction of the reactant or product and ν_i is the viscosity of the reactant or product. The viscosities were converted to diffusion coefficients assuming the Stokes–Einstein relation.[40,108] This method of calculating the viscosity has previously been successfully implemented for modeling of the oxidation of oleic acid.[107] It should also be noted that there is a discrepancy of approximately a factor of seven between the measured viscosity of the 1 : 1 mixture of BA and glutaric acid (C5) and the value required within the model to fit the experimental uptake measurements. This may be due to deviations from the Stokes–Einstein equation, which is expected to occur for viscosities above ~10 Pa s.[108]

Sensitivity studies were performed on all parameters that are summarized in Table 2. The uptake coefficient was sensitive to the surface accommodation coefficient, the surface rate coefficient of reaction (R1), the viscosity of the reactant and the viscosity of Product 1. The surface accommodation determined the initial uptake coefficient at time $t = 0$ and was thus constrained by the measured uptake coefficients at short times. The surface rate coefficient of reaction (R1) and the viscosity of Product 1 determined the availability of glutaric acid (C5) near the surface and were thus jointly responsible for temporal evolution of the uptake coefficient. Sensitivity tests demonstrated that an increase of one order of magnitude in the viscosity of glutaric acid (C5) decreased the modeled uptake coefficient by a maximum of ~10% at the longest reaction times. In contrast, the modeled uptake coefficients were found to be insensitive to the bulk rate coefficient of reaction (R1) and the Henry's law constant of BA, as the uptake was dominated by fast reactions on the surface of the diacid crystal. In addition, the desorption lifetime of BA and the surface rate coefficient of reaction (R1) were found to be co-dependent, such that a decrease in one of these parameters by a certain order of magnitude could be counteracted by increasing the other parameter by the same order of magnitude.

Results and discussion

Fig. 3 shows typical uptake traces for BA on C3–C8 diacids at $[BA]_0$ = (3–5) × 10^{11} cm^{-3}. There was no uptake observed on suberic acid (C8). The difference between the signal intensity with the lid closed compared to when it is open is a measure of the uptake coefficient (eqn (1)). Table 3 summarizes the uptake coefficients for all experiments.

An unexpected trend observed in Fig. 3 is the prolonged steady and repeated uptake when the lid is opened, indicating a lack of surface saturation on both even and odd carbon diacids. Surface saturation commonly occurs with gas–solid reactions such as HNO_3 with NaCl.[99,109–113] Saturation times for BA on the diacids, if it occurs, can be estimated as follows. The rate of reaction of amine molecules with the surface when the Knudsen cell lid is open is equal to the rate of loss of reactive sites:

$$\text{Rate of amine reaction } (cm^{-2}\ s^{-1}) = \text{Rate of loss of reactive sites } (cm^{-2}\ s^{-1})$$

This equality can be rewritten as eqn (4),

$$\frac{k_r}{A_{surf}} N_r = k' S_0 \quad (4)$$

where k_r (s^{-1}) is the first-order rate constant for the amine molecules reacting with a surface, A_{surf} is the reactive surface area of the sample, N_r is the absolute steady-state number of amine molecules while the lid is open, k' (s^{-1}) is the first-order rate constant for the loss of acid reactive sites, and S_0 is the initial number density of the reactive (–COOH) sites per cm^2 of the sample surface. Approximate values of S_0 for malonic (C3) and succinic (C4) acids as examples of odd and even diacids respectively, were both obtained from published unit cell dimensions (each diacid containing 2 molecules per unit cell).[114,115] The dimensions for malonic (C3) acid are a = 0.533 nm, b = 0.514 nm, and c = 1.125 nm.[114] Unit cell dimensions for succinic acid (C4) are a = 0.510 nm, b = 0.888 nm, and c = 0.761 nm.[115] This yields the number of diacid molecules per cm^2 (3.4 × 10^{14} cm^{-2} for malonic acid (C3) and 3.0 × 10^{14} cm^{-2} for succinic acid (C4)). S_0 values are obtained when these surface number densities are weighted by the fraction of surface area that are acidic reactive sites, the latter estimated from layer structures given in Thalladi *et al.*[92] The weighting factor for malonic acid (C3) is 0.25 and for succinic acid (C4) is 0.24. Therefore, for malonic acid (C3) S_0 = 8.5 × 10^{13} cm^{-2} and for succinic acid (C4), S_0 = 7.1 × 10^{13} cm^{-2}.

The first-order rate constant, k_r, can be calculated from measured values and kinetic molecular theory *via* eqn (5),[1]

$$k_r = \gamma \frac{1}{V} A_{surf} \sqrt{\frac{RT}{2\pi M}} \quad (5)$$

where γ is the uptake coefficient (*i.e.*, the fraction of collisions leading to reaction), V is the volume of the Knudsen cell (cm^3), R is the gas constant (kg m^2 mol^{-1} s^{-2} K^{-1}), T is the absolute temperature (K), and M is the molar mass of BA (kg mol^{-1}). Since values of V (691 cm^3), R, T (296 K), and M (7.3 × 10^{-2} kg mol^{-1}) were the same for all experiments, only γ and A_{surf} depend on a

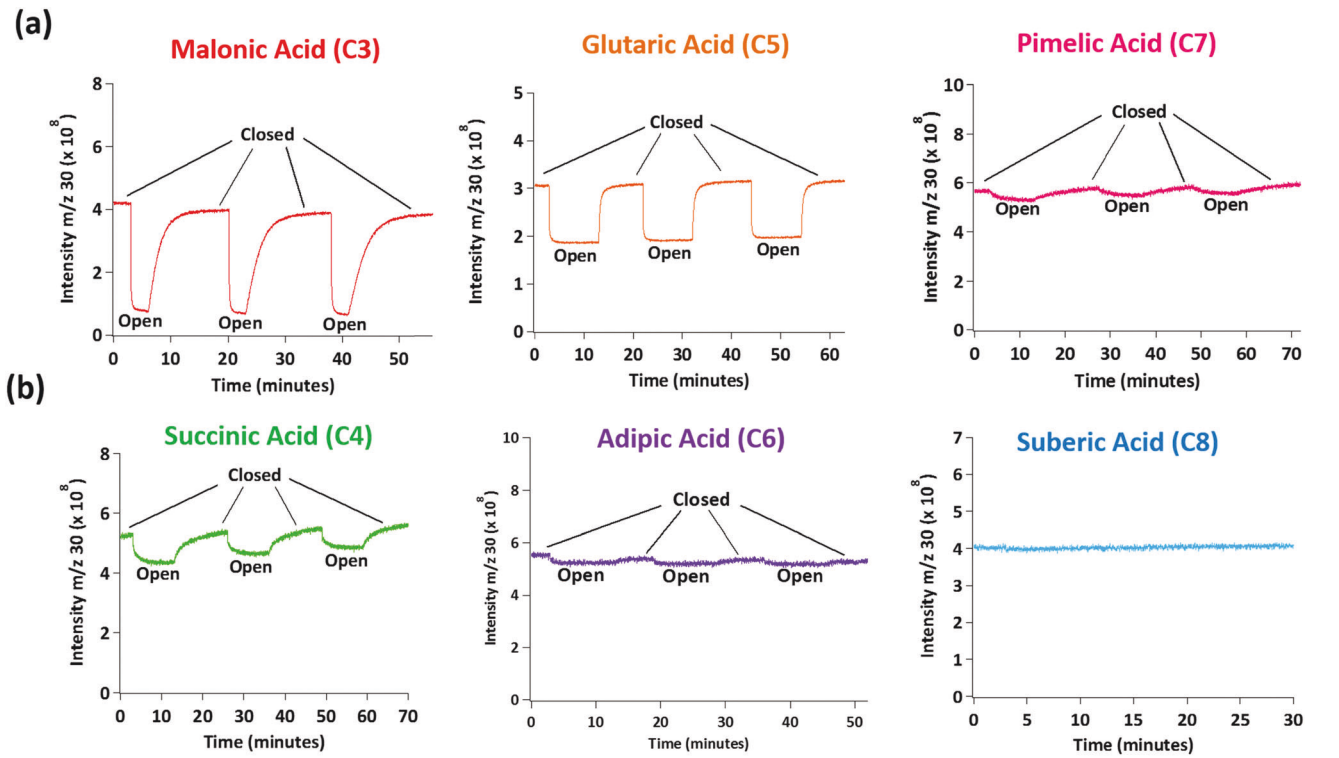

Fig. 3 (a) Uptake profiles for odd carbon diacids: malonic acid (C3), glutaric acid (C5), and pimelic acid (C7). (b) Uptake profiles for even carbon diacids: succinic acid (C4), adipic acid (C6), and suberic acid (C8). $[BA]_0$ = (3–5) × 10^{11} cm^{-3} for all experiments.

Table 3 Uptake coefficients (γ) for different concentrations of *n*-butylamine on different surface areas of diacids

	Surface area (cm^2) $\pm 2\sigma^a$	Orifice area (cm^2)	No. of experiments	$[BA]_0$ (10^{12} cm^{-3}) $\pm 2\sigma^b$	$\gamma \pm 2\sigma^d$
Malonic (C3)	2.0 ± 0.9	0.31	3	0.29[c]	0.65 ± 0.19
	4.2 ± 2.1	0.31	3	0.29[c]	0.60 ± 0.19
	1.8 ± 0.9	0.31	3	4.1 ± 0.2	0.77 ± 0.23
	4.4 ± 2.2	0.31	3	4.9 ± 0.3	0.91 ± 0.27
Succinic (C4)	21.3 ± 6.4	0.015	3	0.49 ± 0.07	$(1.7 \pm 0.6) \times 10^{-4}$[e]
	21.4 ± 5.6	0.015	4	4.9 ± 0.5	$(3.3 \pm 0.9) \times 10^{-4}$[e]
Glutaric (C5)	2.0 ± 0.7	0.31	5	0.32 ± 0.03	0.099 ± 0.026
	4.5 ± 1.5	0.31	6	0.31 ± 0.03	0.11 ± 0.022
	2.1 ± 1.0	0.31	3	3.7 ± 0.2	0.37 ± 0.17[e]
	4.4 ± 9.1	0.31	3	4.1 ± 0.4	0.30 ± 0.14[e]
Adipic (C6)	32.5 ± 15.5	0.015	3	0.44 ± 0.07	$(1.9 \pm 1.4) \times 10^{-5}$[e]
	30.3 ± 12.6	0.015	3	4.2 ± 0.3	$(2.8 \pm 1.9) \times 10^{-5}$[e]
Pimelic (C7)	9.6 ± 4.5	0.015	4	0.45 ± 0.04	$(1.1 \pm 0.54) \times 10^{-4}$[e]
	9.4 ± 5.1	0.015	3	4.4 ± 1.1	$(1.1 \pm 0.64) \times 10^{-4}$[e]
Suberic (C8)	16.0 ± 10.5	0.015	4	0.45 ± 0.05	$\leq 8 \times 10^{-6}$[f]
	14.9 ± 11.6	0.015	3	4.5 ± 0.7	$\leq 6 \times 10^{-6}$[f]

[a] Standard deviations represent 2σ for the distribution of crystal sizes in each sample. [b] Standard deviations represent 2σ for the variation in butylamine concentrations for those runs. [c] Amine concentration for all samples was constant. [d] The errors are statistically determined standard deviations. However, due to the significant uncertainty in particle shape, which affects surface area, the overall uncertainty is estimated to be about a factor of two. [e] Uptake coefficient decreased with time; these values represent the average of the first trial for all samples. [f] Represents an upper limit.

given experiment. For example, using average values from Table 3, k_r was calculated for malonic acid (C3) to be $k_r = 14\ s^{-1}$ (using $\gamma = 0.65$, $A_{surf} = 2.0\ cm^2$, $[BA]_0 = 2.9 \times 10^{11}\ cm^{-3}$) and for succinic acid (C4) $k_r = 3.8 \times 10^{-2}\ s^{-1}$ (using $\gamma = 1.7 \times 10^{-4}$, $A_{surf} = 21.3\ cm^2$, $[BA]_0 = 4.9 \times 10^{11}\ cm^{-3}$).

The absolute steady-state number of amine molecules when the Knudsen cell lid is raised (N_r) can be calculated from experimental data using eqn (6),

$$N_r = V[BA]_0\left(\frac{I_r}{I_0}\right) \quad (6)$$

in which the initial amine concentration before the lid is opened, $[BA]_0$, is reduced by the fractional change in the amine signal once the lid is raised (I_r/I_0). With values of k_r and N_r, and a reasonable estimate of S_0, eqn (4) can be solved for k', the first-order rate constant for reactive site loss. If surface saturation were to occur, then the reactive site density must decay with time as $S_t = S_0 e^{-k't}$. It follows then, that the reciprocal of k', solved from eqn (4), gives the lifetime of reactive sites, τ (s). For representative experiments, we obtain $\tau = 0.3$ s for malonic acid (C3) and $\tau = 145$ s for succinic acid (C4). However, neither malonic (C3) or succinic (C4) acids showed signs of saturation over many minutes of uptake at concentrations of $10^{11}\ cm^{-3}$ (Fig. 3), suggesting that more than the surface is available for reaction. Similar conclusions apply for the rest of the diacids. For comparison, the uptake of amines onto solid ammonium sulfate, bisulfate, nitrate, and chloride salts have been reported to show signs of surface saturation.[116] A limitation on the availability of reactive species at surfaces is also consistent with a size dependence for the replacement of dimethylamine on ammonium bisulfate clusters, where displacement of the ammonium ions from the clusters became more difficult as cluster size increased.[117]

A possible explanation may lie in the nature of the surface formed upon reaction. The interaction of a gas with a solid is initially with the surface layer. If the reaction is restricted to the surface, passivation occurs, effectively shutting down the reaction. However, reaction of the surface layer makes it more disordered and likely more porous. This can allow penetration of incoming gas molecules deeper into the crystal structure. Note also that if surface saturation occurs, the calculated value of the uptake coefficient would be expected to decrease with time. The time for surface saturation would be large at low concentrations and smaller for higher concentrations.

As shown in Fig. 4, odd carbon diacids have much larger uptake coefficients compared to even carbon diacids. Furthermore, within each series (odd or even carbon numbers), the uptake coefficient decreases with increasing chain length. Previous DART-MS (direct analysis in real time mass spectrometry) studies[118] did not find detectable amounts of amines on the surfaces of C4 and C6 diacids, consistent with only a few

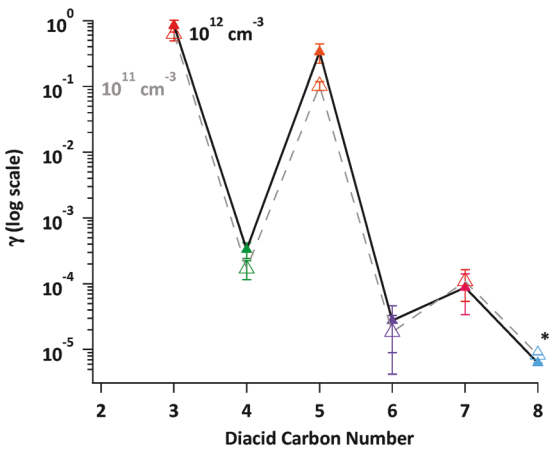

Fig. 4 Summary of initial uptake coefficients, γ, for BA on C3–C8 diacids. Dashed lines are for $10^{11}\ cm^{-3}$ and solid lines are for $10^{12}\ cm^{-3}$. Error bars represent a propagation of errors (2σ). *Uptake coefficients for C8 represent an upper limit.

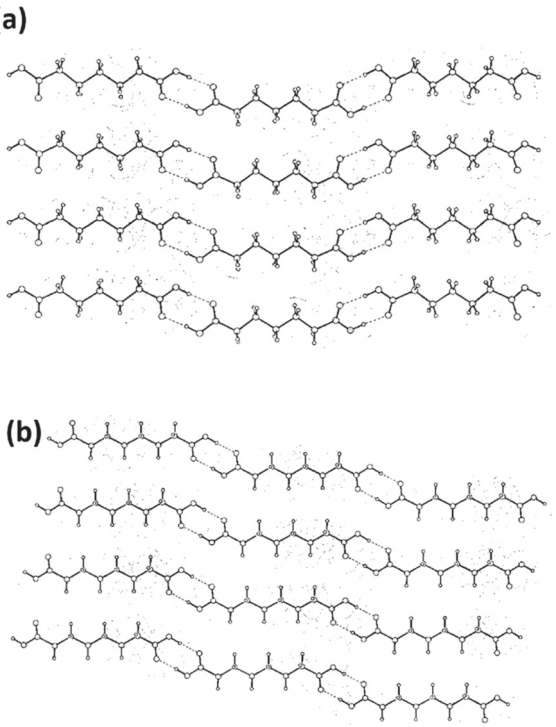

Fig. 5 Arrangement of diacid lattice as reported by Thalladi *et al.*[92] for (a) pimelic acid (C7) and (b) suberic acid (C8). Chains are linked end-to-end *via* hydrogen bonding between –COOH groups and intramolecular chains are held together *via* dispersion forces between methylene groups. The odd carbon diacids have a twisted conformation and more torsional strain than the even carbon diacids.

surface layers being available for reaction. The observations of Zhao *et al.*[118] are also consistent with greater incorporation of the amines into the odd carbon diacid particles, with a trend to decreasing incorporation as the chain lengths increased.

Both even and odd carbon diacids form intramolecular chains bound end-to-end by symmetric hydrogen bonds formed between –COOH end groups. Adjacent chains maintain the crystal structure due to dispersion forces between the methylene groups of the carbon chain as shown in Fig. 5.[92] The decrease in uptake coefficient with increasing chain length within each series is consistent with greater diacid crystal stability due to increased dispersion forces,[92] making it more difficult to disrupt the surface in order to penetrate and react with the crystal lattice, thus leading to less reaction and lower effective uptake coefficients. Malonic acid (C3) has the shortest chain and least dispersion forces; in addition, its crystal structure is triclinic whereas all other diacids are monoclinic,[92] which may change its reactivity compared to the larger diacids.

Odd–even carbon alternations for diacids have been observed in physical properties such as vapor pressure,[95–97] melting point,[92] and solubility.[93,94] One possibility for the increased reactivity of odd carbon diacids is the arrangement and stability of the crystal lattice. The odd carbon diacids adopt a trapezoidal arrangement due to the twisted conformation and torsional strain resulting from packing.[92] Even carbon diacids are offset to minimize interactions between the carboxyl groups and are not twisted, resulting in a more stable parallelogram conformation.[92] These arrangements result in odd carbon diacid lattices having larger spacing in between the diacid chains and being less stable than the even carbon diacid lattices. As a result of the larger spacing, water molecules can more easily disrupt the packing structure of odd carbon diacids, which has been proposed to explain their higher aqueous solubility.[93] A similar effect was seen in their solubility in organic solvents.[94] Thus, butylamine may be able to disrupt the odd carbon lattices in an analogous manner, resulting in the higher reactivity of the odd carbon diacids.

Another contributing factor may be the orientation and thus the availability of the –COOH groups on the surface. Ruehl *et al.*[119] proposed that the orientation of diacids on the surface of aqueous ammonium sulfate particles depended on the diacid structure, with the odd carbon diacids having one –COOH group pointing outside the particle while even carbon diacids have both –COOH groups buried inside the liquid interface. However, these orientations correspond to aqueous particles and the surface structure may not be the same for solid particles.

Finally, the higher uptake coefficients for the odd diacids may be due to the nature of the aminium salts formed during reaction. Salts formed from amines and monocarboxylic acids have been shown to exist as viscous ionic liquids at room temperature.[77] However, aminium dicarboxylate salts formed from methyl-, dimethyl- and trimethylamine with succinic (C4), adipic (C6), and azelaic (C9) acids were solids.[77] To test for the possible formation of ILs on the surface of the dicarboxylic acid in the present experiments, butylaminium salts were synthesized from evaporated 1 : 1 and 2 : 1 molar ratios of aqueous solutions of BA and C3–C8 diacids. Fig. 6a shows that malonic (C3), glutaric (C5), and pimelic (C7) acids all form viscous liquids at room temperature in 2 : 1 BA : diacid molar ratios. For 1 : 1 amine : diacid molar ratios, all three odd carbon diacid mixtures still form viscous liquids (Fig. 6c), although pimelic acid (C7) solidified after several days. Given the ionic nature of the reaction products, these can be considered ionic liquids.[120,121] Measured viscosities for the mixtures from odd carbon diacids are reported in Table 4. For the 1 : 1 mixtures, the longer the diacid chain, the higher the measured viscosity. The trend is not continuous for the 2 : 1 mixtures but the viscosity for the C3 diacid is significantly smaller than for the C5 and C7 diacids. These observations are consistent with previous studies showing higher viscosities for longer carboxylate ions in ammonium-based ionic liquids.[120,121] If the gas–solid reactions form an ionic liquid layer on the surface of these odd carbon diacids in the Knudsen cell, then continued uptake of the amine occurs into a liquid rather than with the surface of a solid. In this case, the underlying diacid may dissolve into the liquid layer, allowing for continuous reaction on one sample without saturation.

This hypothesis was further tested by exposing a sample of malonic acid (C3) crystals to a high concentration of BA in the vacuum manifold. Fig. 7 shows malonic acid (C3) crystals under vacuum before (Fig. 7a) and after (Fig. 7b) exposure to $\sim$41 Torr of BA. The reaction appears to have converted the surface of the malonic acid (C3) crystals into a viscous liquid. Note that although suberic acid (C8) did not form a solid salt from aqueous

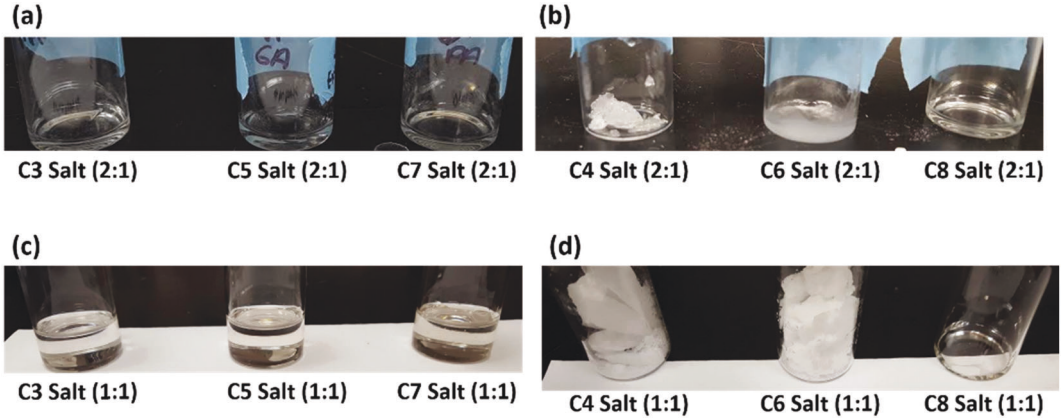

Fig. 6 Formation of liquid and solid salts from aqueous mixtures of *n*-butylamine and diacids. 2 : 1 butylaminium salts for (a) odd carbon diacids and (b) even carbon diacids. 1 : 1 butylaminium salts for (c) odd carbon diacids and (d) even carbon diacids.

Table 4 Measured viscosities (μ) and densities (ρ_f) for 2 : 1 and 1 : 1 amine : diacid mixtures

	2 : 1		1 : 1	
n-Butylamine/ diacid mixture	μ (Pa s) $\pm$ 2σ	ρ_f (units of 10^3 kg m^{-3})	μ (Pa s) $\pm$ 2σ	ρ_f (units of 10^3 kg m^{-3})
Malonic (C3)	11 $\pm$ 0.6	1.1	5 $\pm$ 0.2	1.2
Glutaric (C5)	39 $\pm$ 6	1.1	9 $\pm$ 0.6	1.1
Pimelic (C7)	24 $\pm$ 4	1.0	12 $\pm$ 1.6	1.1

solutions (Fig. 6b and d) as did the other even carbon diacids, the uptake coefficient was too small to be measured (Table 3). When a sample of suberic acid (C8) was exposed to $\sim$29 Torr of BA, a similar phase change was observed (Fig. 7c and d), consistent with the aqueous mixture of amines and diacid remaining liquid. Given that suberic acid (C8) is expected to have the strongest intramolecular dispersion forces and hence the most stable crystal structure of the diacids used in these experiments, the amine may not have enough time to penetrate and disrupt the diacid chains to form the ionic liquid layer under the timescale and amine concentrations of the Knudsen cell experiments. This leads to a small measured uptake coefficient for BA on suberic acid (C8).

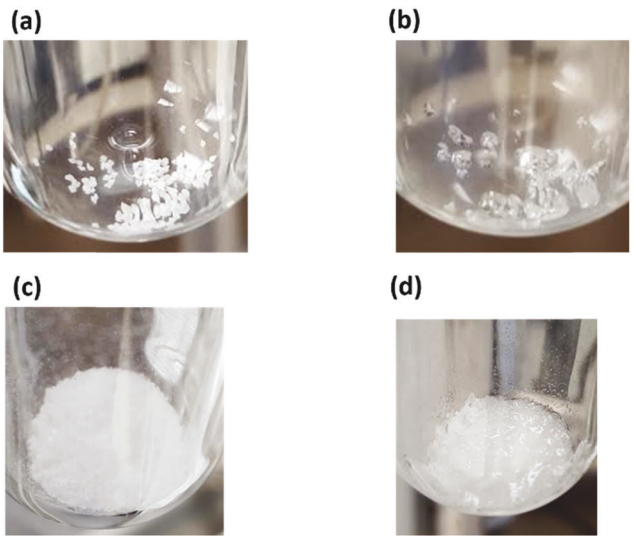

Fig. 7 Malonic acid (C3) (a) before and (b) after exposure to 41 Torr pure *n*-butylamine and suberic acid (C8) (c) before and (d) after exposure to 29 Torr pure *n*-butylamine *via* vacuum manifold.

As shown in Fig. 6b and d, mixtures of both 1 : 1 and 2 : 1 molar ratios of the C4 and C6 diacids with BA formed solid salts rather than ionic liquids. The observed uptake of BA on even carbon diacids in Fig. 3 is far less compared to the odd carbon diacids (Table 3). This is expected if the even carbon diacid salts are solids, while the odd carbon diacid salts are ionic liquids. In the case of solids, the initial reaction of the gas with the surface layer disrupts the packing, leading to a highly defective and more porous surface. The gas then continues to penetrate the surface layer slowly and reacts with underlying layers. The gas–solid reaction described earlier was directed towards reactions that converted gas–solid reactants to a solid product. However, it appears that the products of the reactions of the odd carbon diacids are ionic liquids rather than solid salts. This means that once some number of surface layers have reacted, the surface is no longer a solid, and uptake of the amine is into a liquid layer where diffusion is faster. The measured uptake coefficient will then depend on the true uptake coefficient of the amine onto the liquid, the viscosity of the liquid layer, the dissolution of the underlying solid diacid, and the kinetics of the acid–base reaction in the ionic liquid layer.

Uptake measurements were also carried out in the Knudsen cell at higher BA concentrations, (3–5) $\times$ 10^{12} cm^{-3}. There is a general trend towards higher initial effective uptake coefficients at the higher amine concentrations (Table 3). The results were particularly evident for succinic (C4) and glutaric (C5) acids. In these two cases, the uptake profiles also show signs of surface saturation (Fig. 8 and 9a). The higher uptake coefficients at higher amine concentrations are unexpected, in that for typical gas–solid reactions, higher concentrations generally lead to smaller measured uptake coefficients as the surface becomes passivated more quickly. It may be that in the case of succinic (C4) and adipic (C6) acids (Table 3), which do not form ionic liquids on our time scales, there is a greater disruption of the

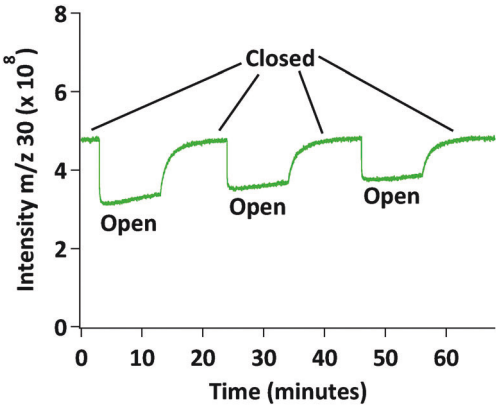

Fig. 8 Uptake of 5×10^{12} cm^{-3} *n*-butylamine on succinic acid ($A_{surf} \sim 21$ cm^2).

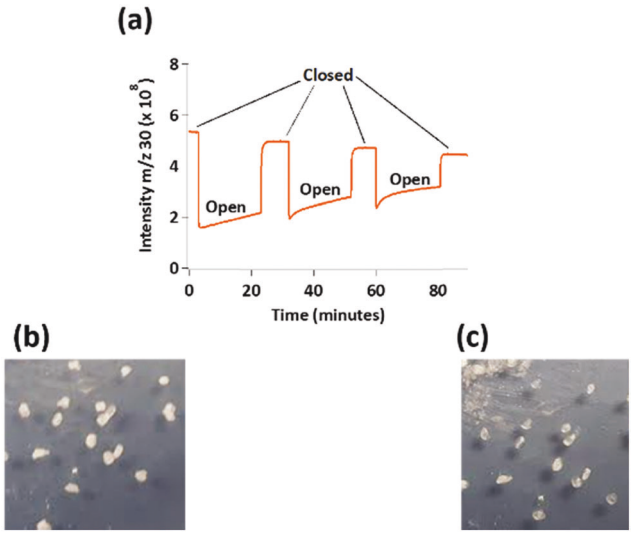

Fig. 9 (a) Uptake profile for 4×10^{12} cm^{-3} *n*-butylamine on glutaric acid ($A_{surf} \sim 2$ cm^2). Glutaric acid (b) before and (c) after reaction in the Knudsen cell with a total exposure time of 60 minutes.

surface and penetration of the amine into the salt at the higher amine concentrations. This would effectively expose more reactive salt for reaction, leading to higher effective uptake coefficients.

In addition to surface saturation, there was also a change in the appearance of the glutaric acid (C5) crystals before and after exposure to the amine (Fig. 9b and c), with the crystal surface appearing more liquid-like at higher amine concentrations. The higher concentration of amine could be forcing the formation of the surface IL layer in the glutaric acid (C5) reaction at a faster rate than at the lower concentrations. If the rate at which the underlying diacid is dissolving into the liquid layer is not sufficiently fast to replenish the diacid compared to the rate at which the amine molecules are being taken up, surface saturation could become evident.

Fig. 10a–c show the measured and KM-SUB modeled uptake coefficients for increasing gas-phase BA concentrations of 3×10^{11} cm^{-3}, 3.9×10^{12} cm^{-3}, and 8.8×10^{12} cm^{-3} on glutaric acid (C5). The model predicts that as BA concentrations increase, the reactive uptake becomes limited by the bulk diffusion of glutaric acid (C5) to the surface.[122] Thus, the uptake coefficient decreases as the diacid reactant becomes depleted near the surface. At the lower BA concentrations, the reactive uptake is dominated by surface reaction limited by surface accommodation of BA, as glutaric acid (C5) is relatively rapidly replenished at the surface in comparison to the loss reaction (R1),[122] leading to a constant uptake coefficient over the reaction time. For the lowest BA concentration, the surface accommodation of BA

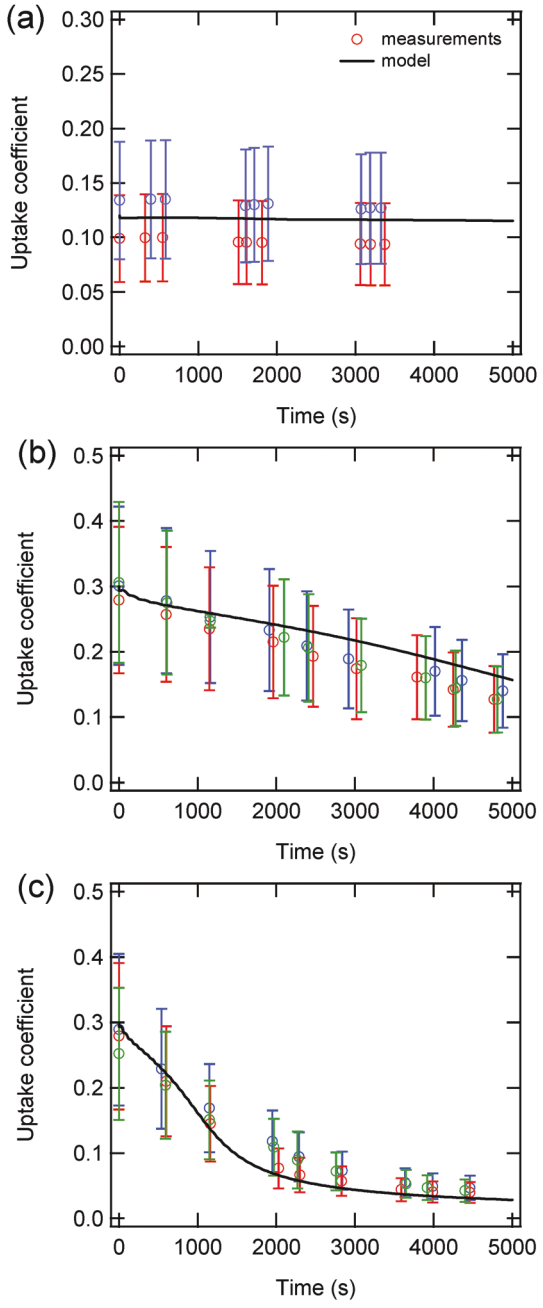

Fig. 10 The measured and modeled uptake coefficient as a function of time for $[BA]_0$ = (a) 3.0×10^{11} cm^{-3}, (b) 3.9×10^{12} cm^{-3} and (c) 8.8×10^{12} cm^{-3} on glutaric acid (C5). The different colors of the markers represent repeats of the experiments.

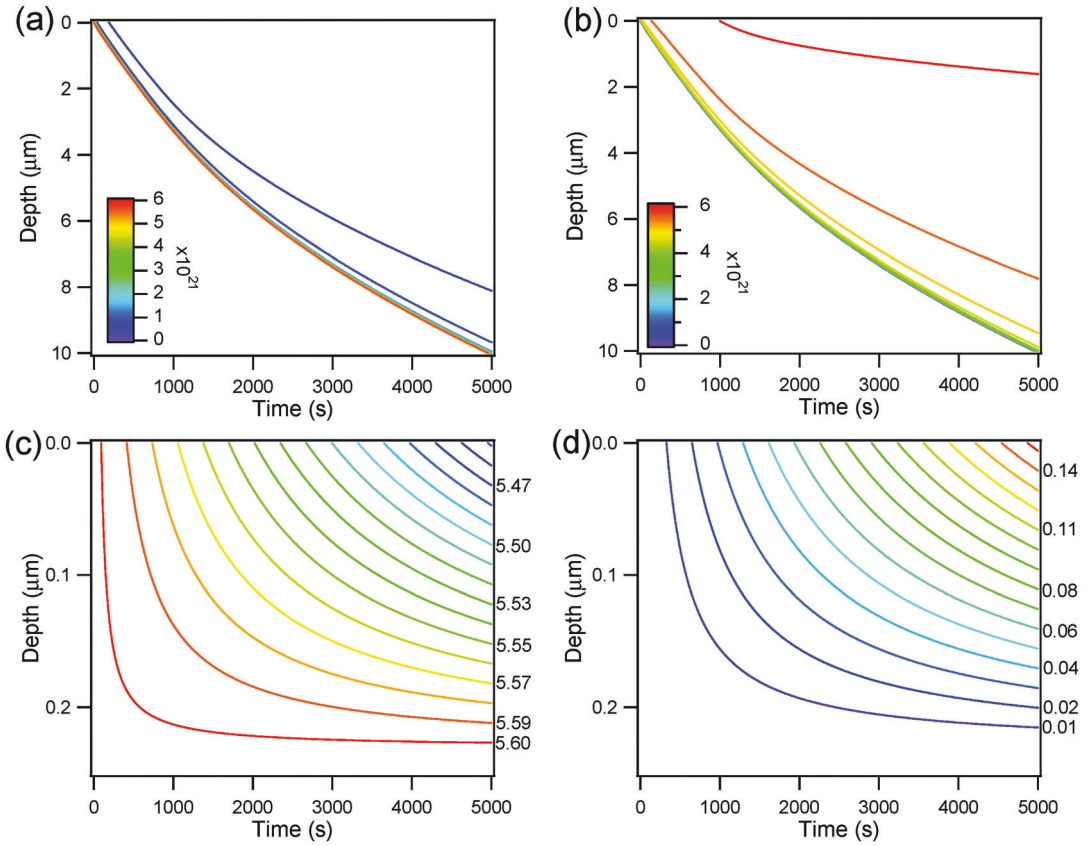

Fig. 11 The temporal evolution of (a) glutaric acid (C5) and (b) reactant product concentrations when exposed to $[BA]_0 = 8.8 \times 10^{12}$ cm^{-3} and the temporal evolution of (c) adipic acid (C6) and (d) reactant product concentrations when exposed to $[BA]_0 = 4.7 \times 10^{12}$ cm^{-3}. Units of the contour lines are cm^{-3}. In panels (c) and (d) the values are in units of 10^{21} cm^{-3}.

was decreased from 0.3 to 0.1 in Fig. 10c to be consistent with the experimental measurements. The smaller value at the lower concentrations is likely due to kinetic limitations in forming the ionic liquid layer over the time scale of the experiments.

Fig. 11 shows the predicted temporal evolution of the reactants and products in the bulk of glutaric (C5) and adipic (C6) acids, when exposed to a BA concentration of 8.8×10^{12} cm^{-3} and 4.7×10^{12} cm^{-3}, respectively. As discussed above, BA and glutaric acid (C5) form an ionic liquid, while BA and adipic acid (C6) form solid salts. Over the experimental time period of 5000 seconds, glutaric acid (C5) concentrations decrease in the 10 μm closest to the surface (Fig. 11a) and the ionic liquid product concentrations increase significantly (Fig. 11b). This is due to the fast reactions of glutaric acid (C5) with BA on the surface and in the near surface bulk of glutaric acid (C5). In comparison, the reaction of BA with adipic acid (C6) was several orders of magnitude slower than the equivalent reaction with glutaric acid (C5), leading to only a small conversion of adipic acid (C6) in the first 0.2 μm of the crystal. This is consistent with the even carbon diacids remaining as solids during the reaction, limiting the availability of the diacid. Note that there is a significant difference in the change in concentration as a function of time for both the diacid and product concentrations for both glutaric (C5) and adipic (C6) acids, with adipic acid (C6) showing very little change over this time scale.

Conclusion

The uptake of butylamine onto low molecular weight diacids (C3–C8) depends on the diacid, with the uptake coefficients being larger for odd carbon diacids than for even carbon homologs. Uptake coefficients also decrease with increasing carbon number in each series. Although the uptake coefficient for malonic acid (C3) approaches unity, the other coefficients are smaller. This may have implications for how atmospheric models treat uptake, even for simple acid–base reactions which have been proposed to play a role in atmospheric particle growth.[10,79]

The hypothesis that the reaction between gaseous BA and solid odd carbon diacids produces ionic liquids in the Knudsen cell is supported by the formation of liquid salts from evaporated 2 : 1 and 1 : 1 aqueous mixtures of BA and the diacids (Fig. 6). It is further supported by the observed liquefaction of the surfaces of solid malonic (C3) (Fig. 7b) and glutaric (C5) (Fig. 9c) acids when exposed to high concentrations of gaseous BA. The lack of surface saturation may be due to the formation of an ionic liquid layer which dissolves the underlying diacid, thus providing a continuous supply of diacid as the amine is taken up from the gas phase. This picture of the gas–solid interactions developed from the experimental data is supported by quantitative modeling using the KM-SUB which incorporates diffusion of viscous reactants

and products through multiple surface layers. Further work is needed to explore reactions of amines of varying structures and properties on the diacids to determine if size and available sites for hydrogen bond formation, for example, affect uptake.

Acknowledgements

This work was supported by the National Science Foundation (Grant #1207112). We thank Professor Heather Allen and Ellen Adams for helpful discussions.

References

1 B. J. Finlayson-Pitts and J. N. Pitts Jr, *Chemistry of the upper and lower atmosphere: theory, experiments, and applications*, Academic Press, 2000.
2 J. H. Seinfeld and S. N. Pandis, *Atmospheric chemistry and physics: from air pollution to climate change*, John Wiley & Sons, 1998.
3 P. J. Ziemann and R. Atkinson, *Chem. Soc. Rev.*, 2012, **41**, 6582–6605.
4 M. Hallquist, J. C. Wenger, U. Baltensperger, Y. Rudich, D. Simpson, M. Claeys, J. Dommen, N. M. Donahue, C. George, A. H. Goldstein, J. F. Hamilton, H. Herrmann, T. Hoffmann, Y. Iinuma, M. Jang, M. E. Jenkin, J. L. Jimenez, A. Kiendler-Scharr, W. Maenhaut, G. McFiggans, T. F. Mentel, A. Monod, A. S. H. Prevot, J. H. Seinfeld, J. D. Surratt, R. Szmigielski and J. Wildt, *Atmos. Chem. Phys.*, 2009, **9**, 5155–5236.
5 N. M. Donahue, A. L. Robinson and S. N. Pandis, *Atmos. Environ.*, 2009, **43**, 94–106.
6 J. H. Seinfeld and J. F. Pankow, *Annu. Rev. Phys. Chem.*, 2003, **54**, 121–140.
7 J. H. Kroll and J. H. Seinfeld, *Atmos. Environ.*, 2008, **42**, 3593–3624.
8 R. Y. Zhang, A. Khalizov, L. Wang, M. Hu and W. Xu, *Chem. Rev.*, 2012, **112**, 1957–2011.
9 M. Kulmala and V. M. Kerminen, *Atmos. Res.*, 2008, **90**, 132–150.
10 I. Riipinen, T. Yli-Juuti, J. R. Pierce, T. Petaja, D. R. Worsnop, M. Kulmala and N. M. Donahue, *Nat. Geosci.*, 2012, **5**, 453–458.
11 W. C. Hinds, *Aerosol Technology: Properties, Behavior and Measurement of Airborne Particles*, John Wiley & Sons Inc., New York, 1999.
12 A. Singh, W. J. Bloss and F. D. Pope, *Atmos. Chem. Phys. Disc.*, 2016, 1–32, DOI: 10.5194/acp-2016-738.
13 D. K. Farmer, C. D. Cappa and S. M. Kreidenweis, *Chem. Rev.*, 2015, **115**, 4199–4217.
14 V. F. McNeill, N. Sareen and A. N. Schwier, Surface-Active Organics in Atmospheric Aerosols, in *Atmospheric and Aerosol Chemistry*, ed. V. F. McNeill and P. A. Ariya, Springer Berlin Heidelberg, Berlin, Heidelberg, 2014, pp. 201–259.
15 M. O. Andreae and D. Rosenfeld, *Earth-Sci. Rev.*, 2008, **89**, 13–41.
16 J. M. Sun and P. A. Ariya, *Atmos. Environ.*, 2006, **40**, 795–820.
17 U. Poschl, *Angew. Chem., Int. Ed.*, 2005, **44**, 7520–7540.
18 V. Ramanathan, P. J. Crutzen, J. T. Kiehl and D. Rosenfeld, *Science*, 2001, **294**, 2119–2124.
19 P. R. Buseck and M. Posfai, *Proc. Natl. Acad. Sci. U. S. A.*, 1999, **96**, 3372–3379.
20 K. Adachi, S. H. Chung and P. R. Buseck, *J. Geophys. Res.: Atmos.*, 2010, **115**, D15206.
21 T. Stocker, D. Qin, G. Plattner, M. Tignor, S. Allen, J. Boschung, A. Nauels, Y. Xia, B. Bex and B. Midgley, *IPCC, 2013: Climate change 2013: The physical science basis. Contribution of working group I to the fifth assessment report of the intergovernmental panel on climate change*, 2013.
22 R. F. Phalen, *Inhalation studies: foundations and techniques*, 1984.
23 G. Oberdorster, Z. Sharp, V. Atudorei, A. Elder, R. Gelein, W. Kreyling and C. Cox, *Inhalation Toxicol.*, 2004, **16**, 437–445.
24 G. Oberdorster, E. Oberdorster and J. Oberdorster, *Environ. Health Perspect.*, 2005, **113**, 823–839.
25 P. M. Mannucci, S. Harari, I. Martinelli and M. Franchini, *Intern. Emerg. Med.*, 2015, **10**, 657–662.
26 M. R. Heal, P. Kumar and R. M. Harrison, *Chem. Soc. Rev.*, 2012, **41**, 6606–6630.
27 C. A. Pope and D. W. Dockery, *J. Air Waste Manage. Assoc.*, 2006, **56**, 709–742.
28 D. W. Dockery, C. A. Pope, X. Xu, J. D. Spengler, J. H. Ware, M. E. Fay, B. G. J. Ferris and F. E. Speizer, *N. Engl. J. Med.*, 1993, **329**, 1753–1759.
29 P. K. Hopke, *Atmos. Environ.*, 2008, **42**, 3192–3194.
30 B. R. Gurjar, A. Jain, A. Sharma, A. Agarwal, P. Gupta, A. S. Nagpure and J. Lelieveld, *Atmos. Environ.*, 2010, **44**, 4606–4613.
31 J. L. Mauderly and J. C. Chow, *Inhalation Toxicol.*, 2008, **20**, 257–288.
32 R. E. Wyzga and A. C. Rohr, *J. Air Waste Manage. Assoc.*, 2015, **65**, 523–543.
33 P. S. J. Lakey, T. Berkemeier, H. J. Tong, A. M. Arangio, K. Lucas, U. Poschl and M. Shiraiwa, *Sci. Rep.*, 2016, **6**, 32916.
34 U. Poschl and M. Shiraiwa, *Chem. Rev.*, 2015, **115**, 4440–4475.
35 J. I. Halonen, T. Lanki, T. Yli-Tuomi, P. Tiittanen, M. Kulmala and J. Pekkanen, *Epidemiology*, 2009, **20**, 143–153.
36 X. X. Tie, D. Wu and G. Brasseur, *Atmos. Environ.*, 2009, **43**, 2375–2377.
37 J. Lelieveld, J. S. Evans, M. Fnais, D. Giannadaki and A. Pozzer, *Nature*, 2015, **525**, 367–371.
38 T. Koop, J. Bookhold, M. Shiraiwa and U. Poschl, *Phys. Chem. Chem. Phys.*, 2011, **13**, 19238–19255.
39 M. Shiraiwa and J. H. Seinfeld, *Geophys. Res. Lett.*, 2012, **39**, L24801.
40 M. Shiraiwa, M. Ammann, T. Koop and U. Poschl, *Proc. Natl. Acad. Sci. U. S. A.*, 2011, **108**, 11003–11008.
41 J. R. Odum, T. Hoffmann, F. Bowman, D. Collins, R. C. Flagan and J. H. Seinfeld, *Environ. Sci. Technol.*, 1996, **30**, 2580–2585.
42 N. M. Donahue, S. A. Epstein, S. N. Pandis and A. L. Robinson, *Atmos. Chem. Phys.*, 2011, **11**, 3303–3318.

43 N. M. Donahue, A. L. Robinson, C. O. Stanier and S. N. Pandis, *Environ. Sci. Technol.*, 2006, **40**, 2635–2643.
44 J. F. Pankow, *Atmos. Environ.*, 1994, **28**, 185–188.
45 J. F. Pankow, *Atmos. Environ.*, 1994, **28**, 189–193.
46 J. F. Pankow, *Atmos. Environ.*, 2015, **122**, 448–453.
47 N. M. Donahue, I. K. Ortega, W. Chuang, I. Riipinen, F. Riccobono, S. Schobesberger, J. Dommen, U. Baltensperger, M. Kulmala, D. R. Worsnop and H. Vehkamaki, *Faraday Discuss.*, 2013, **165**, 91–104.
48 V. Perraud, E. A. Bruns, M. J. Ezell, S. N. Johnson, Y. Yu, M. L. Alexander, A. Zelenyuk, D. Imre, W. L. Chang, D. Dabdub, J. F. Pankow and B. J. Finlayson-Pitts, *Proc. Natl. Acad. Sci. U. S. A.*, 2012, **109**, 2836–2841.
49 C. Kidd, V. Perraud and B. J. Finlayson-Pitts, *Phys. Chem. Chem. Phys.*, 2014, **16**, 22706–22716.
50 C. Kidd, V. Perraud, L. M. Wingen and B. J. Finlayson-Pitts, *Proc. Natl. Acad. Sci. U. S. A.*, 2014, **111**, 7552–7557.
51 M. Shrivastava, A. Zelenyuk, D. Imre, R. Easter, J. Beranek, R. A. Zaveri and J. Fast, *J. Geophys. Res.: Atmos.*, 2013, **118**, 3328–3342.
52 E. Abramson, D. Imre, J. Beranek, J. Wilson and A. Zelenyuk, *Phys. Chem. Chem. Phys.*, 2013, **15**, 2983–2991.
53 C. D. Cappa and K. R. Wilson, *Atmos. Chem. Phys.*, 2011, **11**, 1895–1911.
54 A. Virtanen, J. Joutsensaari, T. Koop, J. Kannosto, P. Yli-Pirila, J. Leskinen, J. M. Makela, J. K. Holopainen, U. Poschl, M. Kulmala, D. R. Worsnop and A. Laaksonen, *Nature*, 2010, **467**, 824–827.
55 A. Zelenyuk, D. Imre, J. Beranek, E. Abramson, J. Wilson and M. Shrivastava, *Environ. Sci. Technol.*, 2012, **46**, 12459–12466.
56 T. D. Vaden, D. Imre, J. Beranek, M. Shrivastava and A. Zelenyuk, *Proc. Natl. Acad. Sci. U. S. A.*, 2011, **108**, 2190–2195.
57 L. Renbaum-Wolff, J. W. Grayson, A. P. Bateman, M. Kuwata, M. Sellier, B. J. Murray, J. E. Shilling, S. T. Martin and A. K. Bertram, *Proc. Natl. Acad. Sci. U. S. A.*, 2013, **110**, 8014–8019.
58 Y. J. Li, P. F. Liu, Z. H. Gong, Y. Wang, A. P. Bateman, C. Bergoend, A. K. Bertram and S. T. Martin, *Environ. Sci. Technol.*, 2015, **49**, 13264–13274.
59 E. Saukko, H. Kuuluvainen and A. Virtanen, *Atmos. Meas. Tech.*, 2012, **5**, 259–265.
60 R. E. O'Brien, A. Neu, S. A. Epstein, A. C. MacMillan, B. B. Wang, S. T. Kelly, S. A. Nizkorodov, A. Laskin, R. C. Moffet and M. K. Gilles, *Geophys. Res. Lett.*, 2014, **41**, 4347–4353.
61 C. N. Jen, P. H. McMurry and D. R. Hanson, *J. Geophys. Res.: Atmos.*, 2014, **119**, 7502–7514.
62 L. Wang, V. Lal, A. F. Khalizov and R. Y. Zhang, *Environ. Sci. Technol.*, 2010, **44**, 2461–2465.
63 H. Yu, R. McGraw and S. H. Lee, *Geophys. Res. Lett.*, 2012, **39**, L02807.
64 T. Berndt, M. Sipila, F. Stratmann, T. Petaja, J. Vanhanen, J. Mikkila, J. Patokoski, R. Taipale, R. L. Mauldin and M. Kulmala, *Atmos. Chem. Phys.*, 2014, **14**, 751–764.
65 J. Zhao, J. N. Smith, F. L. Eisele, M. Chen, C. Kuang and P. H. McMurry, *Atmos. Chem. Phys.*, 2011, **11**, 10823–10836.
66 E. Swartz, Q. Shi, P. Davidovits, J. T. Jayne, D. R. Worsnop and C. E. Kolb, *J. Phys. Chem. A*, 1999, **103**, 8824–8833.
67 S. Schobesberger, A. Franchin, F. Bianchi, L. Rondo, J. Duplissy, A. Kurten, I. K. Ortega, A. Metzger, R. Schnitzhofer, J. Almeida, A. Amorim, J. Dommen, E. M. Dunne, M. Ehn, S. Gagne, L. Ickes, H. Junninen, A. Hansel, V. M. Kerminen, J. Kirkby, A. Kupc, A. Laaksonen, K. Lehtipalo, S. Mathot, A. Onnela, T. Petaja, F. Riccobono, F. D. Santos, M. Sipila, A. Tome, G. Tsagkogeorgas, Y. Viisanen, P. E. Wagner, D. Wimmer, J. Curtius, N. M. Donahue, U. Baltensperger, M. Kulmala and D. R. Worsnop, *Atmos. Chem. Phys.*, 2015, **15**, 55–78.
68 B. Daumer, R. Niessner and D. Klockow, *J. Aerosol Sci.*, 1992, **23**, 315–325.
69 P. H. Mcmurry, H. Takano and G. R. Anderson, *Environ. Sci. Technol.*, 1983, **17**, 347–352.
70 R. C. Robbins and R. D. Cadle, *J. Phys. Chem.*, 1958, **62**, 469–471.
71 A. C. Baldwin and D. M. Golden, *Science*, 1979, **206**, 562–563.
72 J. J. Huntzicker, R. A. Cary and C. S. Ling, *Environ. Sci. Technol.*, 1980, **14**, 819–824.
73 S. M. Murphy, A. Sorooshian, J. H. Kroll, N. L. Ng, P. Chhabra, C. Tong, J. D. Surratt, E. Knipping, R. C. Flagan and J. H. Seinfeld, *Atmos. Chem. Phys.*, 2007, **7**, 2313–2337.
74 S. Angelino, D. T. Suess and K. A. Prather, *Environ. Sci. Technol.*, 2001, **35**, 3130–3138.
75 A. W. Stelson and J. H. Seinfeld, *Atmos. Environ.*, 1982, **16**, 993–1000.
76 Y. C. Liu, Q. X. Ma and H. He, *Environ. Sci. Technol.*, 2012, **46**, 11112–11118.
77 A. Lavi, E. Segre, M. Gomez-Hernandez, R. Y. Zhang and Y. Rudich, *J. Phys. Chem. A*, 2015, **119**, 4336–4346.
78 M. Gomez-Hernandez, M. McKeown, J. Secrest, W. Marrero-Ortiz, A. Lavi, Y. Rudich, D. R. Collins and R. Y. Zhang, *Environ. Sci. Technol.*, 2016, **50**, 2292–2300.
79 T. Yli-Juuti, K. Barsanti, L. Hildebrandt Ruiz, A. J. Kieloaho, U. Makkonen, T. Petaja, T. Ruuskanen, M. Kulmala and I. Riipinen, *Atmos. Chem. Phys.*, 2013, **13**, 12507–12524.
80 X. L. Ge, A. S. Wexler and S. L. Clegg, *Atmos. Environ.*, 2011, **45**, 524–546.
81 K. Kawamura and K. Ikushima, *Environ. Sci. Technol.*, 1993, **27**, 2227–2235.
82 M. P. Fraser, G. R. Cass and B. R. T. Simoneit, *Environ. Sci. Technol.*, 2003, **37**, 446–453.
83 Z. W. Yue and M. P. Fraser, *Atmos. Environ.*, 2004, **38**, 3253–3261.
84 A. Limbeck, Y. Kraxner and H. Puxbaum, *J. Aerosol Sci.*, 2005, **36**, 991–1005.
85 H. Satsumabayashi, H. Kurita, Y. Yokouchi and H. Ueda, *Atmos. Environ., Part A*, 1990, **24**, 1443–1450.
86 A. Limbeck, H. Puxbaum, L. Otter and M. C. Scholes, *Atmos. Environ.*, 2001, **35**, 1853–1862.
87 K. Kawamura, Y. Imai and L. A. Barrie, *Atmos. Environ.*, 2005, **39**, 599–614.
88 S. Saarikoski, S. Carbone, S. Decesari, L. Giulianelli, F. Angelini, M. Canagaratna, N. L. Ng, A. Trimborn, M. C. Facchini,

S. Fuzzi, R. Hillamo and D. Worsnop, *Atmos. Chem. Phys.*, 2012, **12**, 8401–8421.
89 J. N. Smith, K. C. Barsanti, H. R. Friedli, M. Ehn, M. Kulmala, D. R. Collins, J. H. Scheckman, B. J. Williams and P. H. McMurry, *Proc. Natl. Acad. Sci. U. S. A.*, 2010, **107**, 6634–6639.
90 K. A. Pratt, L. E. Hatch and K. A. Prather, *Environ. Sci. Technol.*, 2009, **43**, 5276–5281.
91 Y. Tao, X. N. Ye, S. Q. Jiang, X. Yang, J. M. Chen, Y. Y. Xie and R. Y. Wang, *J. Geophys. Res.: Atmos.*, 2016, **121**, 324–335.
92 V. R. Thalladi, M. Nusse and R. Boese, *J. Am. Chem. Soc.*, 2000, **122**, 9227–9236.
93 H. Zhang, C. Xie, Z. K. Liu, J. B. Gong, Y. Bao, M. J. Zhang, H. X. Hao, B. H. Hou and Q. X. Yin, *Ind. Eng. Chem. Res.*, 2013, **52**, 18458–18465.
94 H. Zhang, Q. X. Yin, Z. K. Liu, J. B. Gong, Y. Bao, M. J. Zhang, H. X. Hao, B. H. Hou and C. Xie, *J. Chem. Thermodyn.*, 2014, **77**, 91–97.
95 C. D. Cappa, E. R. Lovejoy and A. R. Ravishankara, *J. Phys. Chem. A*, 2007, **111**, 3099–3109.
96 M. Bilde, K. Barsanti, M. Booth, C. D. Cappa, N. M. Donahue, E. U. Emanuelsson, G. McFiggans, U. K. Krieger, C. Marcolli, D. Tropping, P. Ziemann, M. Barley, S. Clegg, B. Dennis-Smither, M. Hallquist, A. M. Hallquist, A. Khlystov, M. Kulmala, D. Mogensen, C. J. Percival, F. Pope, J. P. Reid, M. A. V. R. da Silva, T. Rosenoern, K. Salo, V. P. Soonsin, T. Yli-Juuti, N. L. Prisle, J. Pagels, J. Rarey, A. A. Zardini and I. Riipinen, *Chem. Rev.*, 2015, **115**, 4115–4156.
97 M. Bilde, B. Svenningsson, J. Monster and T. Rosenorn, *Environ. Sci. Technol.*, 2003, **37**, 1371–1378.
98 M. Shiraiwa, C. Pfrang and U. Poschl, *Atmos. Chem. Phys.*, 2010, **10**, 3673–3691.
99 P. Beichert and B. J. Finlayson-Pitts, *J. Phys. Chem.*, 1996, **100**, 15218–15228.
100 F. Caloz, F. F. Fenter, K. D. Tabor and M. J. Rossi, *Rev. Sci. Instrum.*, 1997, **68**, 3172–3179.
101 D. M. Golden, G. N. Spokes and S. W. Benson, *Angew. Chem., Int. Ed. Engl.*, 1973, **12**, 534–546.
102 W. Winterbottom and J. Hirth, *J. Chem. Phys.*, 1962, **37**, 784–793.
103 P. Kalsi, *Spectroscopy of organic compounds*, New Age International, 2007.
104 J. R. Taylor, *An introduction to error analysis: the study of uncertainties in physical measurements*, University Science Books, Sausalito, Calif., 2nd edn, 1997.
105 J. B. Franzini, E. J. Finnemore and R. L. Daugherty, *Fluid mechanics with engineering applications*, McGraw-Hill, New York, 9th edn, 1997.
106 D. S. Viswanath, T. Ghosh, D. H. L. Prasad, N. V. K. Dutt and K. Y. Rani, *Viscosity of Liquids*, Springer, 2007.
107 N. A. Hosny, C. Fitzgerald, A. Vysniauskas, A. Athanasiadis, T. Berkemeier, N. Uygur, U. Poschl, M. Shiraiwa, M. Kalberer, F. D. Pope and M. K. Kuimova, *Chem. Sci.*, 2016, **7**, 1357–1367.
108 R. M. Power, S. H. Simpson, J. P. Reid and A. J. Hudson, *Chem. Sci.*, 2013, **4**, 2597–2604.
109 F. F. Fenter, F. Caloz and M. J. Rossi, *J. Phys. Chem.*, 1994, **98**, 9801–9810.
110 J. A. Davies and R. A. Cox, *J. Phys. Chem. A*, 1998, **102**, 7631–7642.
111 R. C. Hoffman, M. A. Kaleuati and B. J. Finlayson-Pitts, *J. Phys. Chem. A*, 2003, **107**, 7818–7826.
112 M. T. Leu, R. S. Timonen, L. F. Keyser and Y. L. Yung, *J. Phys. Chem.*, 1995, **99**, 13203–13212.
113 J. M. Laux, J. C. Hemminger and B. J. Finlayson-Pitts, *Geophys. Res. Lett.*, 1994, **21**, 1623–1626.
114 J. A. Goedkoop and C. H. Macgillavry, *Acta Crystallogr.*, 1957, **10**, 125–127.
115 J. D. Morrison and J. M. Robertson, *J. Chem. Soc.*, 1949, 980–986.
116 Y. Liu, C. Han, C. Liu, J. Ma, Q. Ma and H. He, *Atmos. Chem. Phys.*, 2012, **12**, 4855–4865.
117 B. R. Bzdek, D. P. Ridge and M. V. Johnston, *J. Phys. Chem. A*, 2010, **114**, 11638–11644.
118 Y. Zhao, M. C. Fairhurst, L. M. Wingen, V. Perraud, M. J. Ezell and B. J. Finlayson-Pitts, *Atmos. Meas. Tech. Discuss.*, 2016, 1–34, DOI: 10.5194/amt-2016-357.
119 C. R. Ruehl and K. R. Wilson, *J. Phys. Chem. A*, 2014, **118**, 3952–3966.
120 V. Govinda, P. Venkatesu and I. Bahadur, *Phys. Chem. Chem. Phys.*, 2016, **18**, 8278–8326.
121 T. L. Greaves, A. Weerawardena, C. Fong, I. Krodkiewska and C. J. Drummond, *J. Phys. Chem. B*, 2006, **110**, 22479–22487.
122 T. Berkemeier, A. J. Huisman, M. Ammann, M. Shiraiwa, T. Koop and U. Poschl, *Atmos. Chem. Phys.*, 2013, **13**, 6663–6686.